Philippine Journal of Science
152 (6A): 2129-2137, December 2023
ISSN 0031 - 7683
Date Received: 23 May 2023

Drug-Excipient Compatibility Testing of Cilostazol Using FTIR and DSC Analysis

Syrine Faith Diño[1], Alia Denise Edu[1], Ralph Gean Francisco[1], Emmanuel Gutierrez[1], Perlita Crucis[1,2]*, April Mergelle Lapuz[1], Rogie Royce Carandang[1,3], and Kevin Jace Miranda[1]

[1]College of Pharmacy, Adamson University,
Ermita, Manila, Metro Manila 1000 Philippines
[2]Graduate School, Centro Escolar University,
San Miguel, Manila, Metro Manila 1008 Philippines
[3]Department of Public Health Sciences,
University of Connecticut School of Medicine, Farmington, CT 06030 USA

Cilostazol possesses pharmacological restrictions, such as its absorption being limited by its dissolution rate, and formulation studies must be employed accordingly to generate an optimized formulation. A drug-excipient compatibility analysis is conducted to determine any interactions that may affect the formulation in order to guarantee the stability, bioavailability, and manufacturability of solid dosage forms. To identify any incompatibilities, cilostazol alone and in combination with the individual excipients such as microcrystalline cellulose, crospovidone, magnesium stearate, isopropyl alcohol, sodium lauryl sulfate, polyvinylpyrrolidone K30, and corn starch were subjected to Fourier-transform infrared spectroscopy (FTIR) equipped with an attenuated total reflectance method and heat-flow differential scanning calorimetry (DSC) with a temperature ranging from 30–400 °C at 10 °C/min ramp rate. The FTIR analysis of cilostazol alone and combined with excipients revealed no evidence of chemical or physical instability. Minor changes in the appearance of the absorbance bands in the FTIR comparison can be seen primarily due to the chemical characterization of the excipients, but the characteristic peaks of cilostazol were still present. As for DSC compatibility analysis, the % difference in cilostazol's principal peak temperature alone and with excipients showed no significant change. This implies that no incompatibilities exist between cilostazol and the excipients.

Keywords: drug-excipient interaction, DSC, FTIR

INTRODUCTION

Cilostazol is clinically used to reduce intermittent claudication symptoms of peripheral arterial disease but possesses pharmacological restrictions, wherein its absorption is dissolution rate limited as it is poorly soluble in water (Hiramoto *et al.* 2018). Formulation studies must be employed accordingly to generate an optimized formulation. A drug-excipient compatibility analysis is conducted to determine any instability that may affect the formulation (Veiga *et al.* 2018). This is the initial approach in preformulation studies of drug development to establish an optimal formulation that achieves desirable characteristics in terms of drug stability, bioavailability, and mass-producibility of solid dosage forms (Pani *et al.* 2012).

According to Teleginski and co-authors (2014), drug-excipient compatibility testing is considered to be

*Corresponding author: pcrucis@adamson.edu.ph

the first step in developing a product. Understanding the physicochemical properties of both the active pharmaceutical ingredient (API) and other excipients is important to ensure the safety, efficacy, quality, and stability of the formulated drug. These tests are typically done during the preformulation stages of drug development, wherein the API's characteristics such as melting point and functional groups are noted. Performing compatibility tests early in the development saves the manufacturers from wasting raw materials and time.

In a dosage form, the API and all excipients come in direct contact; thus, any physical or chemical interaction between these two components may negatively impact the stability of the drug, its efficacy, and its appearance. Excipients are added in dosage forms to serve as a vehicle for the API – making a way to administer and absorb the API (Singh *et al.* 2020). They are generally pharmacologically inert; however, excipients could sometimes affect the API chemically (*e.g.* degradation) or physically (*e.g.* increased dissolution time).

Pharmaceutical incompatibility means changes in physical, chemical, and therapeutic properties in a dosage form that occurred, and this was caused by the interaction between the API and the excipients (Dave *et al.* 2015). Determining pharmaceutical incompatibilities plays a very crucial part in formulating pharmaceutical preparations to be able to produce a robust and effective formulation that makes administration easier, improves patient compliance, promotes the release and bioavailability of the drug, and increases its shelf life (Patel *et al.* 2015).

Drug-Excipient Compatibility

Dosage forms contain API and excipients, which are intended to generate an ideal formulation and manufacturability of pharmaceutical products, thereby enabling a much safer and more effective administration (Wang *et al.* 2021). Pharmaceutical excipients are ideally inactive and have no impact on the stability or therapeutic effect of the active ingredient. On the other hand, there are studies that have presented that some excipients are just allegedly described as inactive (Katrajkar *et al*. 2019; Reker *et al.* 2020; Wang *et al.* 2021). Some excipients have the capacity to affect drug efficacy by affecting its pharmacokinetics (Narang *et al.* 2015). Apart from the impact on the drug's therapeutic efficacy, a frequent occurrence of drug-excipient incompatibility is the effect of chemical or physical interactions on the drug's stability (Gorain *et al.* 2018). Excipients can affect the physical and chemical form of pharmaceuticals by several factors such as hydrogen bond interaction, polymorphic conversion, and others (Zhang *et al.* 2018). Accordingly, drug-excipient compatibility should be conducted so as to determine any drug-excipient interactions that may obstruct the stability, bioavailability, and manufacturability of pharmaceutical dosage forms (Chadha and Bhandari 2014; Patel *et al.* 2015).

Cilostazol structure. The structure of cilostazol (Figure 1) consists of a lactam that is 3,4-dihydroquinolin-2(1H)-one with a 4-(1-cyclohexyl-1H-tetrazol-5-yl)butoxy group substituted on the hydrogen at carbon 6 (NCBI 2021).

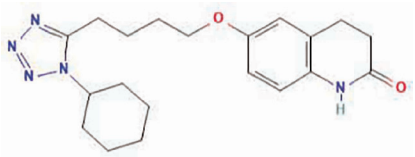

Figure 1. Structure of cilostazol.

Excipients. Excipients are additive substances used to improve the bulkiness, disintegration, dissolution rate, and bioavailability of a formulation. These must be physiologically and chemically stable, must not have any incompatibility with the API, and must meet the standards of regulatory requirements, as per Karthik (2016).

The proposed formulation consists of excipients like disintegrants, lubricants, wetting agents, fillers, and a granulating agent specific for wet granulation. The disintegrants used in the formulation of cilostazol, according to Sawafta and co-authors (2021), are crospovidone and microcrystalline cellulose (MCC). Crospovidone or cross-linked vinylpyrrolidone is a water-insoluble superdisintegrant made by polymerizing vinylpyrrolidone. Unlike other disintegrants, which mainly work by swelling, crospovidone facilitates rapid disintegration by wicking or absorbing liquid (*i.e.* saliva) into the tablet, and due to its highly porous nature, it also swells in water rapidly without gelling (Mohanachandran *et al.* 2011). MCC, with the brand name Avicel, is a diluent with great binding properties and the preferred binder for direct compression. It is self-disintegrating due to its high intraparticle porosity, and it has a low coefficient of friction, making it easier to form into a tablet. MCC is sensitive to hydrophobic lubricants like magnesium stearate (MgSt), which is also common in tablet formulation (Thoorens *et al.* 2014). MgSt is widely used as a lubricant, an important part of tablet formulations, due to its excellent properties and its capability to form films on other pharmaceutical excipients, which extends the drug liberation time and increases disintegration time, as per Zarmpi and co-authors (2020). In line with this, Calahan (2020) stated that lubricants are commonly added in order to prevent granule adherence and improve granule flow properties.

Moreover, isopropyl alcohol (IPA) is used as a granulating agent, and it was shown that the permeability and

compressibility results of IPA indicate that it creates more porous granules and has superior compressibility to water granules (Chaudhari and Dave 2015). For sodium lauryl sulfate (SLS), which is also used as a tablet lubricant and wetting agent, incorporating it into the formulation was found to considerably increase the dissolution rate of a drug, as stated by Alshora and co-authors (2022). While polyvinylpyrrolidone (PVP) is a water-soluble synthetic polymer that is inert, non-toxic, pH stable, and temperature-resistant, which can be used for both hydrophilic and lipophilic API (Dun *et al*. 2018; Kurakula and Rao 2020). The grade of PVP used in the formulation is K30. As a tablet filler used to make up the volume of the tablet, if the tablet is inadequate to produce the desired volume, corn starch is commonly used for its nontoxic and non-irritant properties at a low cost, making it one of the most used diluents in tablet formulation (Builders and Arhewoh 2016).

FTIR and DSC analysis. Fourier-transform infrared spectroscopy (FTIR) is a technique for determining variations within the mixture of drug excipients. In this analysis, the position of the functional groups and their structure observed in the active ingredient and studied excipients are compared (Budiul *et al.* 2017; Canbay *et al.* 2019). The disappearance of an absorption peak, peak intensity reduction, or the appearance of additional peaks will all indicate the presence of interactions of cilostazol, the API, with the excipients being studied (Segall 2019).

On the other hand, differential scanning calorimetry (DSC) is a thermoanalytical method that determines the variation in energy supplied for the sample substance and the temperature-dependent reference material, enabling the evaluation of changes in enthalpy when being heated or cooled (Dourado 2019; Xie *et al.* 2022).

MATERIALS AND METHODS

Study Design

This study used quantitative-experimental research as its approach, in which numerical data produced from the experiments were gathered and analyzed.

Chemicals and Reagents

The procurement of the active ingredient and excipients used for the FTIR and DSC were purchased, as shown in Table 1 with their grades and sources.

Table 1. List of raw materials/chemicals/reagents used.

Raw materials/ chemicals/ reagents	Grade	Source
Cilostazol (raw material)	United States Pharmacopeia (USP)	Xi'an Henrikang Biotech Co., Ltd.
Microcrystalline cellulose (MCC)	USP	Pharmatechnica Laboratory Inc.
Crospovidone	N/A	Compact Pharmaceutical
Magnesium stearate (MgSt)	Extra pure	Aishite Trading Corp.
Isopropyl alcohol (IPA)	Analytical grade	Belman Laboratories
Sodium lauryl sulfate (SLS)	85% Extra pure	Belman Laboratories
Polyvinylpyrrolidone K30 (PVP K30)	N/A	Pharmatechnica Laboratory Inc.
Corn starch	N/A	Belman Laboratories

FTIR

Perkin-Elmer Spectrum Version 10.03.05 (Spectrum Two, PIKE Technologies) at Chemistry Laboratory of Adamson University in Ermita, Manila, Metro Manila was used to obtain the FTIR spectra through the attenuated total reflectance (ATR) method (Zapata *et al.* 2021). The ATR crystal was cleaned with IPA and Kimwipes™ before placing a small amount of freshly prepared cilostazol alone and in combination with excipients on top of the crystal. The screw-type pressure head was used to apply a small amount of pressure, except for the sample of cilostazol with IPA since it is a liquid sample.

DSC

The cilostazol alone and in combination with excipients were subjected to a heat-flow DSC (Perkin-Elmer DSC 4000) at the ADMATEL-DOST (Advanced Device and Materials Testing Laboratory–Department of Science and Technology) in Bicutan, Taguig, Metro Manila. These individual samples were freshly prepared and weighed using an analytical balance of approximately 5.0 mg. The pressure regulator was adjusted to maintain purge gas pressure at 2.0–3.0 bar. The temperature was set ranging from 30–400 °C at 10 °C/min ramp rate. The samples were then loaded into the DSC chamber to analyze, and the data were processed using the Pyris Software. The following formula of the relative percentage difference (RPD) was used for the determination of any incompatibilities (Govindaraja *et al.* 2023):

$$RPD = \left| \frac{R_1 - R_2}{\left(\frac{R_1 - R_2}{2} \right)} \right| \text{ x } 100$$

where:

R1 = peak of the standard (cilostazol)
R2 = peak of the sample (cilostazol with the individual excipients)

Data Analysis

Descriptive statistics was used for the presentation of the data collected in FTIR and DSC.

RESULTS

FTIR Analysis

The FTIR spectrum graph of cilostazol alone showed C-H stretch peaks starting from 2935–3175 cm^{-1}, which correspond to both aliphatic and aromatic groups in cilostazol (Fernandes *et al.* 2020). The vibration peaks around 3175 cm^{-1} indicate the N-H stretching of quinolone. The prominent peak at 1666 cm^{-1} corresponds to the C=N bond of the tetrazole. At 1504 cm^{-1}, the N=N bond present in tetrazole can be observed. Additionally, the peak at 1243 cm^{-1} corresponds to the C-O stretch present in cilostazol (Flourence *et al.* 2020).

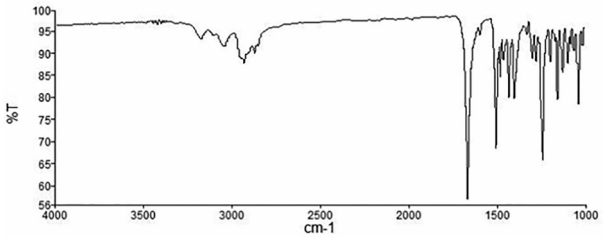

Figure 2. FTIR spectrum of cilostazol.

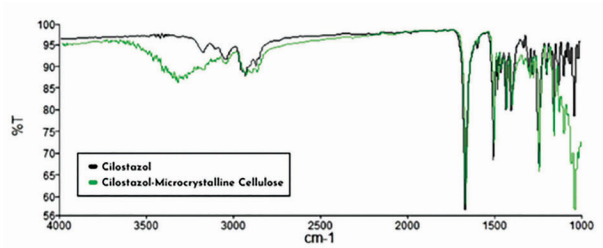

Figure 3. FTIR comparison of cilostazol and cilostazol-MCC.

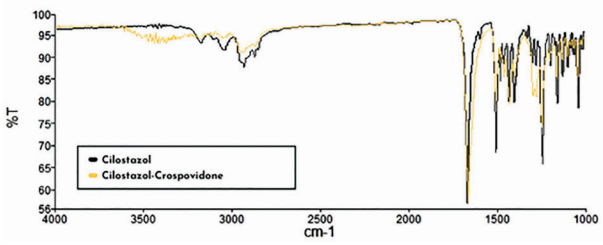

Figure 4. FTIR comparison of cilostazol and cilostazol-crospovidone.

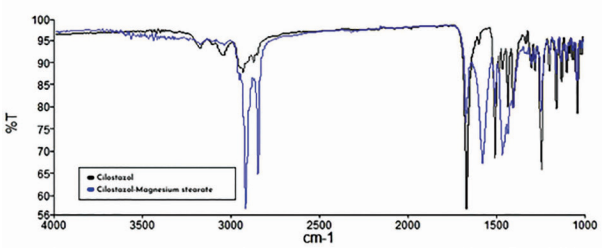

Figure 5. FTIR comparison of cilostazol and cilostazol-MgSt.

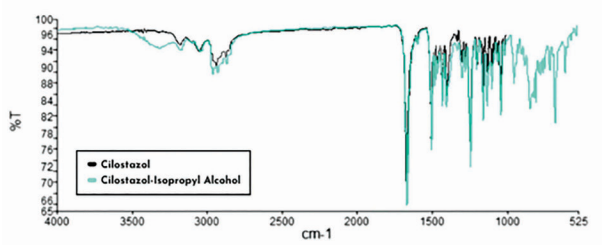

Figure 6. FTIR comparison of cilostazol and cilostazol-IPA.

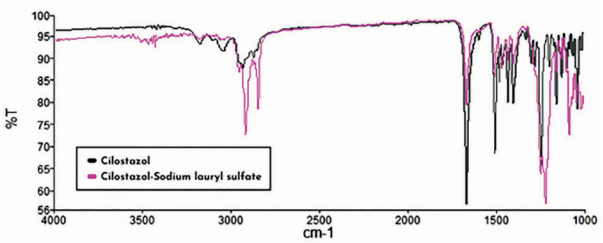

Figure 7. FTIR comparison of cilostazol and cilostazol-SLS.

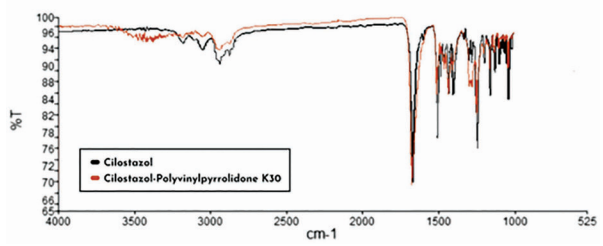

Figure 8. FTIR comparison of cilostazol and cilostazol-PVP K30.

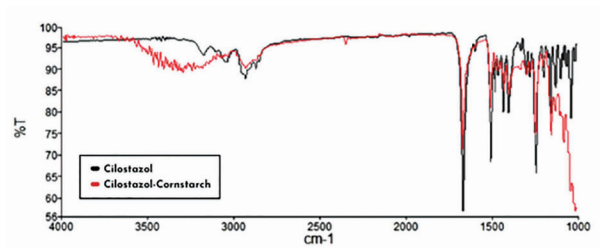

Figure 9. FTIR comparison of cilostazol and cilostazol–corn starch.

The FTIR comparison of cilostazol alone and cilostazol in combination with the individual excipients (MCC, crospovidone, MgSt, IPA, SLS, PVP K30, and corn starch) showed minor changes in the appearance and position of the absorbance bands, which can be primarily due to chemical characterization of the excipients, but the characteristic peaks of cilostazol were still present.

Specifically, Figure 2 shows the spectra of cilostazol alone and Figure 3-9 for cilostazol in combination with the excipients. In MCC, the vibration peaks around 3250–3400 cm^{-1} are present due to surface hydroxyls present in MCC. A noticeable change in the peak around 2800–2934 cm^{-1} is due to stretching vibration of C-H in the pyranoid ring, and 1037–1155 cm^{-1} peaks are due to the C-O stretch of MCC (Wu *et al.* 2014). There are no significant changes in the peaks between cilostazol and cilostazol-MCC combination; thus, it can be assumed that there are no incompatibilities between cilostazol and MCC. No significant changes in the peaks between the cilostazol and cilostazol-crospovidone combination are observed, which means that there are no incompatibilities, as the vibration peaks at 3424–3455 cm^{-1} in the cilostazol-crospovidone spectrum are due to O-H stretching, and the peaks around 2950 cm^{-1} demonstrated the occurrence of asymmetric stretching of CH_2 present in crospovidone (Mireles *et al.* 2020). The broad band at 3452 cm^{-1} in the cilostazol-MgSt spectrum is due to OH stretching vibrations present in the combined carboxyl of MgSt. Noticeable peaks at 2918–2850 cm^{-1} are primarily due to C-H stretching in the CH_2-CH_3 bond present in the molecule of MgSt. In the twin peaks at 1567 and 1464 cm^{-1}, the occurrence of an asymmetric and symmetric stretching vibration, respectively, is evident that corresponds to the carboxylate (COO-) group (Nep and Conway 2011). Thus, it still indicates the absence of interaction between the cilostazol-MgSt combination.

Furthermore, the spectrum of IPA and cilostazol shows no significant interactions as the noticeable peaks around 3178 cm^{-1}, according to Smith (2018), corresponding to the O-H stretch present in IPA, and no significant band changes are observed except for the peaks in the fingerprint region. As per cilostazol and SLS, its spectrum shows prominent peaks between 2849 and 2916 cm^{-1} corresponding to the aliphatic C–H stretching in dodecyl (Nandiyanto *et al.* 2019). Additionally, SLS demonstrated a definite peak of a sulfate group –OSO3- stretching at 1217 and 1081 cm^{-1}. The appearance of a distinct peak at 1243 cm^{-1} indicates the presence of molecular interaction. This implies that the –S=O groups of SLS interacted with the C-O groups of cilostazol since SLS includes electron-donating centers and the C-O of cilostazol has potential electron-accepting centers, as per Zuo and co-authors (2017). In the spectra of cilostazol alone and cilostazol-PVP K30, the vibration peaks around 3400 cm^{-1} are due to the presence of O-H stretch in PVP K30, which indicates the moisture was detected, showing the hygroscopic nature of PVP K30 (El Maghraby and Elsergany 2014). Slight changes in the peak around 1600 cm^{-1} are due to the carbonyl group present in PVP K30. No significant changes were observed in the spectra; hence, there are no incompatibilities between cilostazol and PVP K30. Lastly, the peaks between cilostazol and cilostazol–corn starch combination have elicited vibration peaks around 3299–3450 cm^{-1}, which are present due to hydroxyl groups present in the corn starch. The peaks around 1000–1154 cm^{-1} are due to the C-O bonds in C-O-H and C-O-C groups in the anhydroglucose ring of the corn starch (Kibar and Us 2014).

DSC Analysis

In Figure 10, the DSC spectra of cilostazol alone (A) and in combination with the excipients – MCC (B), corn starch (C), MgSt (D), SLS (E), PVP K30 (F), and crospovidone (G) – showed a main endothermic peak at 161.85 °C, which corresponds to the melting point of cilostazol. As per Table 2, the % RPD in the main peak of cilostazol in combination with the excipients (MCC, crospovidone, MgSt, SLS, PVP K30, and corn starch) as compared with cilostazol alone are as follows: cilostazol-MCC having 0.56% RPD, cilostazol-crospovidone having 1.76%, cilostazol-MgSt having 0.89%, cilostazol-SLS having 2.45%, cilostazol-PVP K30 having 4.11%, and cilostazol–corn starch having 0.51%. However, cilostazol in combination with IPA was not done in the DSC analysis since the sample may evaporate prior to completing the analysis, as pure IPA has a boiling point lower than water and has a tendency to evaporate at room temperature.

Table 2. Thermal behavior of cilostazol and cilostazol + excipients.

Ingredient	Main peak temperature (endothermic)	% RPD[a]
Cilostazol	161.85 °C	–
Cilostazol + microcrystalline cellulose	160.95 °C	0.5576
Cilostazol + crospovidone	164.73 °C	1.7637
Cilostazol + magnesium stearate	160.42 °C	0.8875
Cilostazol + sodium lauryl sulfate	157.94 °C	2.4454
Cilostazol + polyvinylpyrrolidone K30 (PVP K30)	168.64 °C	4.1091
Cilostazol + corn starch	161.03 °C	0.5079

[a]Relative percentage difference

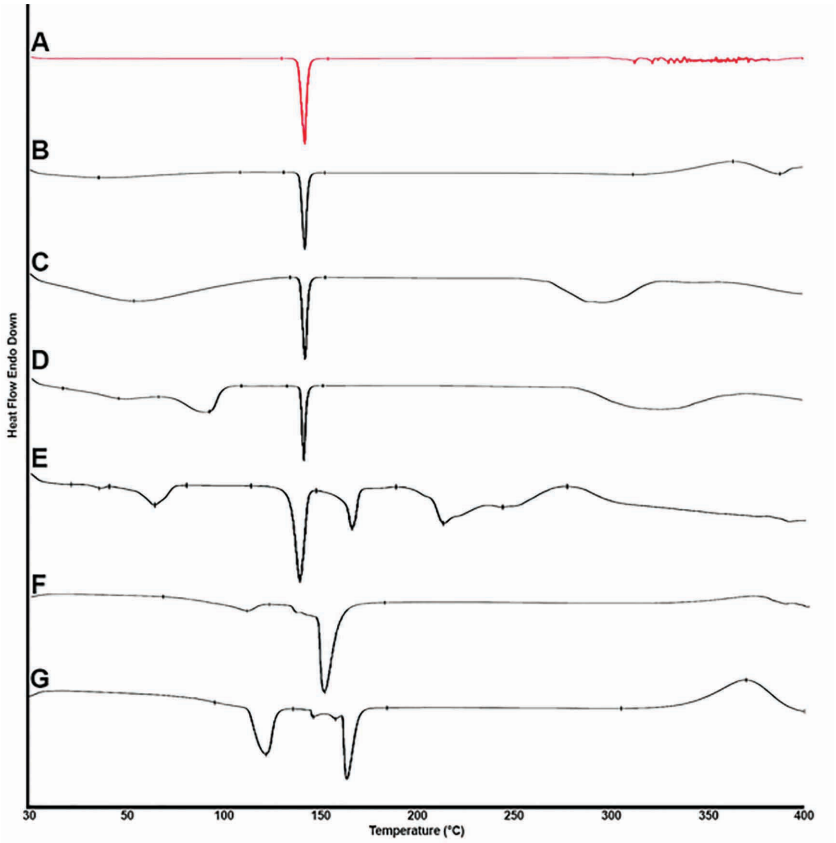

Figure 10. DSC spectra of cilostazol alone and in combination with individual excipients.

DISCUSSION

The FTIR spectra comparison of cilostazol-alone and in combination with the excipients showed no significant changes or differences – only minor changes that correspond to the chemical characteristics of the excipients. Thus, it can be assumed that there are no incompatibilities between cilostazol and the excipients.

As for the DSC analysis, the RPD percent of the cilostazol's principal peak temperature alone and in combination with its excipients also showed no significant change (Raam Dheep and Sreekumar 2018; ASEAN 2018). This indicates that cilostazol did not decompose, degrade, or react poorly in combination with the excipients. Thus, it can be concluded that there are no incompatibilities between cilostazol and the individual excipients.

Hence, the results in both FTIR and DSC mean that cilostazol – when combined with the excipients MCC, crospovidone, MgSt, IPA, SLS, PVP K30, and corn starch – revealed no incompatibilities.

CONCLUSION

Cilostazol is compatible with the following excipients: MCC, crospovidone, MgSt, IPA, SLS, PVP K30, and corn starch. No incompatibilities between the API and the excipients mean they can be formulated together to produce a stable and good-quality pharmaceutical preparation that ensures consistency in terms of stability, bioavailability, and manufacturability of cilostazol dosage forms.

ACKNOWLEDGMENTS

This study was supported by the Center for Research and Development. The authors would also like to thank Ms. Angeli Ann S. Rescober, Mr. Florence V. Marquez, and Ms. Romalyn A. Joson for their assistance with the chemicals and reagents and guidance with the usage of equipment.

REFERENCES

ALSHORA DH, IBRAHIM MA, ZAYED G, AL RWASHED MA, ABOU-TALEB HA, ALI, MF. 2022. The role of sodium lauryl sulfate on formulation of

directly compressed tablets containing simvastatin and aspirin: Effect on drugs dissolution and gastric mucosa. Saudi Pharmaceutical Journal 30(5): 635–645.

[ASEAN] Association of Southeast Asian Nations. 2018. ASEAN Guideline on stability study of drug product. Retrieved on 10 Oct 2022 from https://asean.org/wp-content/uploads/2018/01/25PPWG-ANNEX-7-iv-Final-ASEAN-Guideline-on-Stability-Study-Drug-Product-R2.pdf

BUDIUL M, ALBU P, VLASE G, TURCUŞ V, VLASE T. 2017. Thermogravimetric and calorimetric studies performed on memantine hydrochloride to determine its thermal behaviour and possible drug-excipient interactions. Journal of Thermal Analysis and Calorimetry 127: 555–564.

BUILDERS PF, ARHEWOH MI. 2016. Pharmaceutical applications of native starch in conventional drug delivery. Starch – Stärke 68(9–10): 864–873.

CALAHAN JL. 2020. Correlating the physicochemical properties of magnesium stearate with tablet dissolution and lubrication. Theses and Dissertations–Pharmacy 117.

CANBAY HS, POLAT M, DOĞANTÜRK M. 2019. Study of stability and drug-excipient compatibility of estriol. Bilge International Journal of Science and Technology Research 3(2): 102–107.

CHADHA R, BHANDARI S. 2014. Drug-excipient compatibility screening—role of thermoanalytical and spectroscopic techniques. Journal of Pharmaceutical and Biomedical Analysis 87: 82–97.

CHAUDHARI SP, DAVE RH. 2015. To prepare and characterize microcrystalline cellulose granules using water and isopropyl alcohol as granulating agents and determine its end-point by thermal and rheological tools. Drug Development Industrial Pharmacy 41(5): 744–752.

DUN J, OSEI-YEBOAH F, BOULAS P, LIN Y, SUN CC. 2018. A systematic evaluation of dual functionality of sodium lauryl sulfate as a tablet lubricant and wetting enhancer. International Journal of Pharmaceutics 552(1–2): 139–147.

DAVE VS, HAWARE RV, SANGAVE NA, SAYLES M, POPIELARCZYK M. 2015. Drug-excipient compatibility studies in formulation development: current trends and techniques. American Association of Pharmaceutical Scientists (AAPS) Formulation Design and Development (FDD) Section Newsletter. p. 9–15.

DOURADO D. 2019. Thermal analysis as a useful tool in drug-excipient compatibility studies: The impact in pharmaceuticals products. Biomedical Journal of Scientific and Technical Research 22(3).

EL MAGHRABY GM, ELSERGANY RN. 2014. Fast disintegrating tablets of nisoldipine for intra-oral administration. Pharmaceutical Development and Technology 19(6): 641–650.

FERNANDES AV, PYDI CR, VERMA R, JOSE J, KUMAR L. 2020. Design, preparation and *in vitro* characterizations of fluconazole loaded nanostructured lipid carriers. Brazilian Journal of Pharmaceutical Sciences 56(2).

FLOURENCE T, MALYADRI T, THEJOMOORTHY K, SCREENIVASA PRASANNA P. 2020. Enhancement of dissolution of cilostazole by complexation method using cyclodextrins. World Journal of Current Medical and Pharmaceutical Research 2(2): 166–170.

GORAIN B, CHOUDHURY H, PANDEY M, MADHESWARAN T, KESHARWANI P, TEKADE RK. 2018. Drug-excipient interaction and incompatibilities. Dosage Form Design Parameters. p. 363–402.

GOVINDARAJA G, DURAIPANDI S, SREEKUMAR A. 2023. Development and characterization of a novel eutectic mixture with stearyl alcohol and adipic acid for hot air storage applications. Journal of Energy Storage. p. 61.

HIRAMOTO JS, TERAA M, DE BORST GJ, CONTE MS. 2018. Interventions for lower extremity peripheral artery disease. Nature Reviews Cardiology 15: 332–350.

KARTHIK VV. 2016. Excipients used in the Formulation of Tablets. Research and Reviews: Journal of Chemistry 5: 143–154.

KATRAJKAR K, DARJI L, KETHAVATH D, THAKKAR S, KSHIRSAGAR B, MISRA M. 2019. Shedding light on interaction of so-called inactive ingredients (excipients) with permeability-glycoprotein. Journal of Drug Delivery Science and Technology 52: 531–552.

KIBAR EAA, US F. 2014. Evaluation of structural properties of cellulose ether-corn starch based biodegradable films. International Journal of Polymeric Materials and Polymeric Biomaterials 63(7): 342–351.

KURAKULA M, RAO GSNK. 2020. Pharmaceutical assessment of polyvinylpyrrolidone (Pvp): as excipient from conventional to controlled delivery systems with a spotlight on COVID-19 inhibition. Journal of Drug Delivery Science and Technology 60: 102046.

MIRELES LK, WU M, SAADEH N, YAHIA L, SACHER E. 2020. Physicochemical characterization of polyvinyl pyrrolidone: A tale of two polyvinyl pyrrolidones. ACS Omega 5(47): 30461–30467.

MOHANACHANDRAN PS, SINDHUMOL P, KIRAN TS. 2011. Superdisintegrants: an overview. International journal of pharmaceutical sciences review and research 6: 105–109.

NANDIYANTO AB, OKTIANI R, RAGADHITA R. 2019. How to read and interpret FTIR spectroscopy of organic material. Indonesian Journal of Science and Technology 4(1): 97.

NARANG AS, YAMNIUK A, ZHANG L, COMEZOGLU SN, BINDRA DS, VARIA SA, DOYLE M, BADAWY S. 2015. Drug excipient interactions. Excipient Applications in Formulation Design and Drug Delivery. p. 13–35.

[NCBI] National Center for Biotechnology Information. 2021. PubChem Compound Summary for CID 2754, Cilostazol. Retrieved on 03 Nov 2022 from https://pubchem.ncbi.nlm.nih.gov/compound/Cilostazol

NEP EI, CONWAY BR. 2011. Preformulation studies on grewia gum as a formulation excipient. Journal of Thermal Analysis and Calorimetry 108: 197–205.

PANI NR, NATH L, BHUNIA B. 2012. Application of DSC, IST, and FTIR study in the compatibility testing of nateglinide with different pharmaceutical excipients. Journal of Thermal Analysis and Calorimetry 108(1): 219–226.

PATEL P, AHIR K, PATEL V, MANANI L, PATEL C. 2015. Drug-excipient compatibility studies: first step for dosage form development. The Pharma Innovation Journal 4: 14–20.

RAAM DHEEP G, SREEKUMAR A. 2018. Investigation on thermal reliability and corrosion characteristics of glutaric acid as an organic phase change material for solar thermal energy storage applications. Applied Thermal Engineering 129: 1189–1196.

REKER D, SHI Y, KIRTANE AR, HESS K, ZHONG GJ, CRANE E, LIN CH, LANGER R, TRAVERSO G. 2020. Machine learning uncovers food- and excipient-drug interactions. Cell Reports, Vol. 30.

SAWAFTA O, ALHADID S, ABU AWWAD A, MIGDADI E, ALJABERI A. 2021. Impact of the manufacturing technique on the dissolution-enhancement functionality of PEG4000 in cilostazol tablets. Pharmacia 68: 243–250.

SEGALL AI. 2019. Preformulation: the use of FTIR in compatibility studies. Journal of Innovations in Applied Pharmaceutical Science 4(3): 01–06.

SINGH SY, SALWA, SHIRODKAR RK, VERMA R, KUMAR L. 2020. Enhancement in Dissolution Rate of Atorvastatin Trihydrate Calcium by Formulating Its Porous Tablet Using Sublimation Technique. Journal of Pharmaceutical Innovation 15: 498–520.

SMITH B. 2018. Infrared spectral interpretation: a systematic approach. Boca Raton, FL: CRC Press 1: 71–72.

TELEGINSKI LK, MACIEL AB, MENDES C, SILVA MA, BERNARDI LS, DE OLIVEIRA PR. 2014. Fluconazole-excipient compatibility studies as the first step in the development of a formulation candidate for biowaiver. Journal of Thermal Analysis and Calorimetry 120: 771–781.

THOORENS G, KRIER F, LECLERCQ B, CARLIN B, EVRARD B. 2014. Microcrystalline cellulose, a direct compression binder in a quality by design environment—a Review. International Journal of Pharmaceutics 473: 64–72.

VEIGA A, OLIVEIRA PR, BERNARDI LS, MENDES C, SILVA MAS, SANGOI MS, JANISSEK PR, MURAKAMI FS. 2018. Solid-state compatibility studies of a drug without melting point. Journal of Thermal Analysis and Calorimetry 131: 3201–3209.

WANG N, SUN H, DONG J, OUYANG D. 2021. Pharmde: a new expert system for drug-excipient compatibility evaluation. International Journal of Pharmaceutics 607: 120962.

WU LM, TONG DS, ZHAO LZ, YU WH, ZHOU CH, WANG H. 2014. Fourier transform infrared spectroscopy analysis for hydrothermal transformation of microcrystalline cellulose on montmorillonite. Applied Clay Science 95: 74–82.

XIE X, CHANG Z, CHEN C, ZHANG L, WANG M, TANG C, XUE H, GAO X. 2022. Physicochemical characterization of three active pharmaceutical ingredients for compound glycyrrhizin solid formulation and compatibility analysis *via* thermal and non-thermal techniques. Journal of Pharmaceutical Innovation 17(4): 595–609.

ZAPATA F, LÓPEZ-FERNÁNDEZ A, ORTEGA-OJEDA F, QUINTANILLA G, GARCÍA-RUIZ C, MONTALVO G. 2021. Introducing ATR-FTIR spectroscopy through analysis of acetaminophen drugs: Practical lessons for interdisciplinary and Progressive Learning for undergraduate students. Journal of Chemical Education 98: 2675–2686.

ZARMPI P, FLANAGAN T, MEEHAN E, MANN J, FOTAKI N. 2020. Impact of magnesium stearate presence and variability on drug apparent solubility based on drug physicochemical properties. The AAPS Journal 22(4): 11–18.

ZHANG K, PELLETT JD, NARANG AS, WANG YJ, ZHANG YT. 2018. Reactive impurities in large and small molecule pharmaceutical excipients – a review. TrAC Trends in Analytical Chemistry 101: 34–42.

ZUO W, QU W, LI N, YU R, HOU Y, LIU Y, GOU G, YANG J. 2017. Fabrication of multicomponent amorphous bufadienolides nanosuspension with wet milling improves dissolution and stability. Artificial Cells, Nanomedicine, and Biotechnology 46(7): 1513–1522.